Pakistan Veterinary Journal

ISSN: 0253-8318 (PRINT), 2074-7764 (ONLINE)
DOI: 10.29261/pakvetj/2025.008

RESEARCH ARTICLE

Melatonin Modulates Necroptosis and Enhances Antioxidant Defense during PGF-Induced Luteal Regression in Heat-Exposed Rats

Hadi Tavakolikazerooni[1], Muhammad Tariq[1], Hao Yu[1], Saif Ullah[1], Wael Ennab[2] and Dagan Mao[1]*

[1]College of Animal Science and Technology, Nanjing Agricultural University, Nanjing 210095, China
[2]College of Animal Science and Technology, Yangzhou University, Yangzhou 225009, PR China
*Corresponding author: maodagan@njau.edu.cn

ARTICLE HISTORY (24-733)

Received: November 15, 2024
Revised: February 5, 2025
Accepted: February 6, 2025
Published online: February 17, 2025

Key words:
Female rats
Heat exposure
Luteal regression
Melatonin
Necroptosis
Ovarian function
Oxidative stress

A B S T R A C T

This study was planned to investigate the protective effects of melatonin against heat stress on the reproductive health, focusing on ovarian function and luteal regression. Specifically, it examined the pathways of necroptosis during luteal regression induced by prostaglandin $F_{2\alpha}$ (PGF) in heat-exposed rats. Seventy-five immature female Sprague-Dawley rats were hormonally primed intra-peritoneally with Pregnant Mare's Serum Gonadotropin (PMSG) and human Chorionic Gonadotropin (hCG). After 24h, the rats were divided into three groups (n=25 per group): Non-Heat Exposure (NHE); rats were housed under standard conditions. Heat Exposure (HE); rats were exposed to 41°C for 2h daily for 7 days. Melatonin+Heat Exposure (M+HE); rats were exposed to the same heat conditions as the HE group, with melatonin was administered intra-peritoneally at 10mg/kg body weight. On Day 7, all rats were injected intra-peritoneally with PGF, and euthanized at 0, 2, 8, 16, or 24h post-PGF injection (n=5 on each time point). Blood samples were collected for serum progesterone analysis, and ovaries were harvested for Transmission Electron Microscopy, immunohistochemistry and Western blot analysis. The results revealed that heat stress caused significant down-regulation of steroidogenic proteins (HSD3B and CYP11A1) and elevated necroptotic markers (RIPK1 at 16h, RIPK3 and p-RIPK3 at 24h) post-PGF treatment. Heat exposure also reduced superoxide dismutase (SOD) and catalase (CAT) activities and elevated malondialdehyde (MDA) levels. Conversely, melatonin treatment restored steroidogenic protein expression (StAR and CYP11A1), increased SOD and CAT activities, decreased MDA levels, and reduced necroptosis markers (particularly RIPK3 and p-RIPK3 levels at 16 and 24h). These findings demonstrate the cytoprotective role of melatonin in countering heat-affected luteal regression through modulation of RIPK1/RIPK3 signaling, antioxidant defense enhancement, and preservation of steroidogenesis.

To Cite This Article: Tavakolikazerooni H, Tariq M, Yu H, Ullah S, Ennab W, and Mao D, 2025. Melatonin Modulates Necroptosis and Enhances Antioxidant Defense during PGF-Induced Luteal Regression in Heat-Exposed Rats. Pak Vet J, 45(1): 205-215. http://dx.doi.org/10.29261/pakvetj/2025.008

INTRODUCTION

The corpus luteum (CL) is an atypical endocrine organ that secretes progesterone hormone (P4), which is required for early establishment and continuation of pregnancy (Góes *et al.*, 2022). If conception does not occur, the CL undergoes luteolysis, which helps to restore cyclic ovarian activity. In ruminants, the luteolysis is induced by prostaglandin $F_{2\alpha}$ (PGF) liberated by the uterus (Pate and Hughes, 2023); In rodents, PGF analogues will cause functional and structural regression of the CL (Monaco and Davis, 2023). Apoptosis, especially the caspase-dependent pathway, has been considered the major form of cell death during luteolysis. Recent studies propose that necroptosis, a form of programmed necrotic cell death, may be involved in the pathogenesis of this process (Hojo *et al.*, 2019; Hojo *et al.*, 2022).

Environmental stressors, for instance heat stress, have been shown to exert adverse effects on the reproductive health of any population. Heat stress impairs structural integrity and disrupts hormonal secretion by CL, resulting in poor reproductive performance through reduced serum P4 levels, early pregnancy loss and infertility (Krishnan *et*

al., 2017; Ullah *et al.*, 2019). Moreover, it may delay luteal regression by stimulating the release of P4 in pseudo-pregnant rats (Bai *et al.*, 2017). This effect is further compounded by oxidative stress, which finally lowers fertility and impairs cellular functionality (Butt *et al.*, 2019; Nanas *et al.*, 2021). Necroptosis has been shown to participate in heat-induced cytotoxicity through heat shock proteins to activate Z-DNA-binding protein1 (ZBP1), leading to cell death and membrane breakage (Jiao *et al.*, 2020). Unlike apoptosis, necroptosis is a sort of programmed necrosis that takes place when caspase channels are blocked (Vandenabeele *et al.*, 2010). It is controlled by receptor-interacting protein kinases 1 and 3 (RIPK1/3). Under stress, this protein works as the external mode of cell death called necroptosis (Huang *et al.*, 2021; Morgan and Kim, 2022). Heat exposure has been shown to cause necroptosis through ZBP1, and therefore cell death through membrane disruption (Jiao *et al.*, 2020).

Melatonin is a potent anti-inflammatory antioxidant that has been extensively investigated for its effects on different physiological processes in the animal body, including the reproductive system. Melatonin, originating from the immune cells and pineal gland, is required in immune modulation, regulation of the biological clock, and as an antioxidant to scavenge the free radicals (Chrustek and Olszewska-Słonina, 2021; Ahmad *et al.*, 2023). It is also involved in the various reproductive processes in numerous mammals, from the control of the estrous cycle and follicular growth to implantation of developing embryo (Yong *et al.*, 2021). Previous research shows that it may protect reproductive organs from heat stress (Jiang *et al.*, 2021; Reiter and Sharma, 2021). Melatonin inhibits necroptosis in pathological processes like cardiac ischemia and liver fibrosis through modulating RIPK3-dependent signaling (Yang *et al.*, 2018; Zhou *et al.*, 2018). These properties support melatonin to be used as a promising therapeutic agent in countering heat-induced reproductive damage.

We hypothesized that necroptosis plays a major role in CL cell death during PGF-induced luteolysis under heat stress and that melatonin can mitigate this process by modulating RIPK-dependent pathways. This study aimed to evaluate the role of necroptosis in CL regression under heat stress and to assess the protective effects of melatonin in a rat model. Our findings are expected to provide critical insights into the therapeutic potential of melatonin in mitigating heat-induced reproductive damage.

MATERIALS AND METHODS

Ethical approval: This animal study protocol was approved by the Animal Care and Use Committee of Nanjing Agricultural University, Nanjing, China, with approval Number of SYXK2022-0031.

Animals: A total of 75 immature female Sprague-Dawley rats, aged three weeks with body weight of 50±5g, specific pathogen-free (SPF level), were acquired from the Laboratory Animal Center of Nanjing Agricultural University, China. Rats were maintained under standard conditions (25°C, 12-hour light/dark cycle) with unrestricted access to water and food.

Design of experiments: Following a 7-day acclimatization period, these 75 rats (aged 28 days) were injected intraperitoneally 30 IU of Pregnant Mare's Serum Gonadotropin (PMSG, Folligon, Ningbo Sansheng Biological Technology Co., Ltd., China), followed by 30 IU of human Chorionic Gonadotropin (hCG, Chorulon, Ningbo Sansheng Biological Technology) 48h later, as previously described (Bai *et al.*, 2017; Tang *et al.*, 2021). Twenty-four hours post-hCG administration (designated Day 0), rats were assigned to three groups (n = 25 each): (1) Non-Heat Exposure (NHE): Rats were housed under standard conditions. (2) Heat Exposure (HE): Rats were exposed to heat (41°C for 2h daily) for seven consecutive days. (3) Melatonin+Heat Exposure (M+HE): Rats were exposed to the same heat conditions as the HE group, along-with the melatonin treatment.

Heat stress was induced by placing rats in temperature-controlled chambers with a heating element, maintaining an ambient temperature of 41°C for 2h daily, from 11:00AM to 1:00PM, over seven consecutive days (Bai *et al.*, 2017). To ensure the safety and well-being of the rats, the chambers were equipped with sufficient space to allow uniform heat exposure, and an oxygen enhancer was incorporated to maintain adequate oxygen levels during the heat exposure. All rats in the heat-exposed group tolerated the treatment without any observed complications. Melatonin (Cat. No.: HY-B0075, MedChem Express) was dissolved in a vehicle solution (0.9% saline with 1% ethanol) at a concentration of 2mg/mL. The M+HE group received daily i.p. injections of melatonin at a dosage of 10mg/kg body weight at 9:00 AM for seven days, as described previously (Mojaverrostami *et al.*, 2019).

On Day 7, following a 2-hour recovery period post-heat exposure, rats in all groups (n=25 per group) received an i.p. injection of 0.3mL PGF (Cloprostenol, a synthetic PGF2α analogue, 0.1mg/mL, Ningbo Sansheng Pharmaceutical) to induce luteolysis. Rats of the control group received 0.9% saline at the 0-hour time point. Rats were euthanized by ether inhalation at 0, 2, 8, 16, or 24h post-PGF injection (n=5 on each time point) for temporal data collection.

Blood samples without anticoagulant were collected immediately after euthanasia at each time point. One ovary from 3 rats per time point was preserved in 4% paraformaldehyde for histological examination and immunohistochemistry to assess structural changes and protein localization, while one ovary from 2 rats per time point was fixed in 2.5% glutaraldehyde for ultrastructural analysis using Transmission Electron Microscopy (TEM). The second ovary from 5 rats per time point was used for Western blotting (WB) to evaluate protein expression related to necroptosis, luteal function and assessment of antioxidant enzyme activity. This allocation ensured a comprehensive assessment while adhering to ethical and methodological standards.

Progesterone assay: To obtain serum, the blood was left to clot at room temperature for 2h, followed by centrifugation at 4000g for 10 minutes. A radioimmunoassay (RIA) kit (B08JFB; National Institute of Biological Sciences, Beijing, China) at Nanjing Xinfan Biotechnology Co., Ltd. was used to assess serum

progesterone concentrations. Assay sensitivity was 0.2ng/mL, with intra-assay CV of <10% and inter-assay CV of <15%.

Antioxidant enzyme activities: Catalase (CAT) activity was measured using the catalase activity assay kit from Solarbio Science & Technology Co., Ltd., Beijing, China. The assay was conducted based on the manufacturer's instructions. Catalase reacts with methanol in the presence of hydrogen peroxide, producing formaldehyde which is measured spectrophotometrically at 540nm. Catalase activity was quantified in units per milligram of protein (U/mg protein), defined as the amount of enzyme decomposing 1.0μmole of hydrogen peroxide per minute at pH 7.0 and 25°C. Serum and tissue samples were processed to normalize enzyme activity based on protein concentrations determined by the Bradford protein assay (Hadwan *et al.*, 2024).

Superoxide dismutase (SOD) activity was assessed using a kit from Biotime Biotechnology Co., Ltd., Haimen, China, utilizing the water-soluble tetrazolium salt (WST-1) method (Yang *et al.*, 2020). This method measures the inhibition of formazan dye formation by SOD, indicating the enzyme activity in reducing the superoxide anion generated by a xanthine oxidase system. Absorbance was recorded at 450nm, with activity expressed in units per milligram of protein (U/mg protein); one unit corresponded to the enzyme amount necessary for 50% dismutation of the superoxide radical. The manufacturer's protocol was followed in the assay for both serum and tissue samples.

Malondialdehyde (MDA) levels were determined using the MDA Content Assay Kit from Solarbio Science & Technology Co., Ltd. The assay quantifies MDA by its reaction with thiobarbituric acid, forming a measurable complex at 532nm (Liu *et al.*, 2020). MDA content was expressed in micromoles per liter (μmol/L). Following the manufacturer's instructions, the assay was performed on both serum and tissue samples to evaluate oxidative stress.

Western blot analysis: Western blotting was performed, as reported earlier (Yu *et al.*, 2023). Ovaries were homogenized in radio-immuno-precipitation assay (RIPA) buffer (Beyotime, Institute of Biotechnology, Jiangsu, China) containing 10mM phenylmethylsulphonyl fluoride (PMSF; Beyotime). Total proteins were obtained by centrifugation of samples at 12,000g for 20 minutes at 4°C. The resulting pellets were discarded. The bicinchoninic acid (BCA) assay kit (Beyotime) was used to measure protein content, and equal amounts of protein were loaded onto 10% sodium dodecyl sulfate (SDS)–polyacrylamide gels. Proteins were then transferred to polyvinylidene difluoride (PVDF) membranes (Millipore, Bedford, MA, USA) and blocked with 5% bovine serum albumin (BSA) in Tris-buffered saline Tween-20 (TBST) for 90 minutes at room temperature. Subsequently, membranes were incubated with specific primary antibodies (Table 1) overnight at 4°C. Following three washes for 5 minutes each with TBST, membranes were incubated with appropriate horseradish peroxidase-conjugated secondary antibodies for 2h at room temperature. Finally, membranes were detected using an enhanced chemiluminescence (ECL) system (Chemistar Highsig ECL Western Blotting Substrate; Tanon, Nanjing, China). Protein bands were visualized using a Luminescent Image Analyzer LAS4000 (Fuji Film, Tokyo, Japan) and the integrated light intensity for each band was quantified using ImageJ software (ImageJ, version 1.54d, National Institutes of Health, Bethesda, MD, USA).

Table 1: Antibodies utilized in the study for Western Blotting (WB)

Antibodies	CAT No.	Supplier	Antigen source	Host	Dilution (WB)
α-Tubulin					
β-Actin	AC007	Abclonal	Human	Rabbit	1: 3000
CYP11A1	AC004	Abclonal	Human	Mouse	1: 5000
GAPDH	A16363	Abclonal	Human	Rabbit	1: 1000
HSD3B	AC002	Abclonal	Human	Mouse	1: 5000
p-RIPK1(RIP-S166)	A1823	Abclonal	Human	Rabbit	1: 1000
p-RIPK3(Ser316)	AP1230	Abclonal	Human	Rabbit	1: 1000
RIPK1	AF4508	Affinity	Human	Rabbit	1: 1000
RIPK3	A7414	Abclonal	Human	Rabbit	1: 1000
StAR	A5431	Abclonal	Human	Rabbit	1: 1000
HRP Anti-M IgG	A1035	Abclonal	Human	Rabbit	1: 1000
(secondary)	AS014	Abclonal	Rabbit	Goat	1: 10000
HRP Anti-R IgG	AS003	Abclonal	Mouse	Goat	1: 10000
(secondary)					

Immunohistochemistry: Immunohistochemistry (IHC) was performed following the protocol described previously (Yu *et al.*, 2023). Briefly, ovary samples, embedded in paraffin wax, were sectioned into 5μm slices. Sections were then deparaffinized in xylene, followed by rehydration through a descending series of ethanol solution. Subsequently, endogenous peroxidase activity was nullified by treatment with 0.3% H_2O_2. To mitigate non-specific binding, sections were blocked with 5% BSA for 1h at room temperature. Sections were subjected to overnight incubation at 4°C with primary antibodies using RIPK1 Rabbit pAb (A7414, Abclonal) at dilution of 1:50 and RIPK3 Rabbit pAb (A5431, Abclonal) at dilution of 1:100. Specific protein immunoreactivity was visualized using a streptavidin biotin-peroxidase complex (SABC) kit (Boster Biological Technology, Wuhan, China). Sections were then stained with 3,3-diaminobenzidine (DAB; Sigma-Aldrich, St Louis, MO, USA) to serve as the chromogen. As a negative control, PBS was employed instead of the primary antibody. The images were captured using a Nikon YS100 microscope (Nikon, Tokyo, Japan) equipped with a digital camera (Model D3300; Nikon) and ImageJ software (ImageJ, version 1.54d, National Institutes of Health, Bethesda, MD, USA), which featured an IHC profiler compatible plug-in, was used for analysis.

Transmission electron microscopy: Transmission Electron Microscopy (TEM) was carried out using the procedure outlined previously (Ullah *et al.*, 2019). For this purpose, luteal tissues were immersed in 2.5% glutaraldehyde in PBS (pH 7.4) at 4°C, then post-fixed with 1% osmium tetroxide (Sigma-Aldrich, Merck, UK), dehydrated, and embedded in Araldite. Sections (0.06μm) were produced using a Reichert Ultra Cut E ultramicrotome, stained using Reynold's lead citrate and uranyl acetate, followed by observation with a Philips CM-120 electron microscope.

Statistical analysis: Data are expressed as mean±SEM. Statistical analyses were performed using SPSS

software (version 17.0; SPSS Inc., USA). The primary aim of the analysis was to assess temporal variations within individual groups and to compare differences among treatment groups at corresponding time points. One-way ANOVA, followed by Tukey's post-hoc test was employed for pairwise comparisons. Where appropriate, two-way ANOVA was used to evaluate the interaction effects between time points and treatment groups. A P<0.05 was considered statistically significant.

RESULTS

Effects of melatonin and heat exposure on serum progesterone and ovarian steroidogenic protein expression: Progesterone levels were assessed at multiple time points after PGF injection (Fig. 1). Following PGF treatment, a sharp decline in progesterone concentration was observed across all groups (NHE, HE, and M+HE), which remained low until 16h. At 24h, progesterone levels rebounded in all groups; however, the levels in the NHE and HE groups remained significantly lower than their 0-h values (P<0.05). In contrast, the M+HE group showed no difference in serum progesterone levels between 0 and 24h, suggesting that melatonin mitigated the prolonged suppression of progesterone. Notably, the M+HE group showed significantly reduced progesterone levels at 2h (P<0.05) but elevated at 24h in comparison with the HE group (P<0.05; Fig. 1).

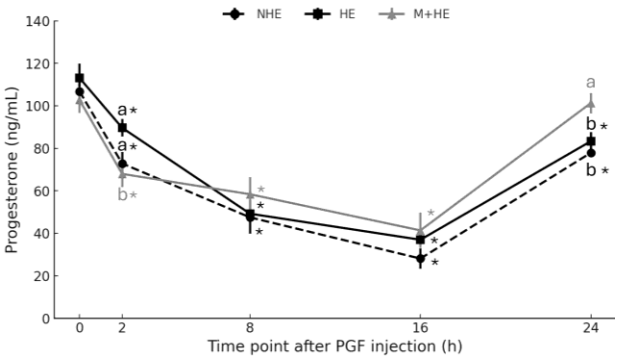

Fig. 1: Effects of melatonin on serum progesterone levels in heat-exposed rats at various time points post-PGF injection. The figure presents a two-way ANOVA, showing the effects of groups (NHE, HE, M+HE), time points, and their interaction on serum progesterone levels. P-values for the group effect (P=0.046), time effect (P<0.01), and interaction effect (P=0.028) are displayed on the plot. Statistical significance of progesterone concentrations within the same group over time is indicated by an asterisk (*), and comparisons among groups are annotated with p-values. Data are expressed as means±SEM from 5 rats per time point.

To assess the impact of melatonin and heat exposure on mechanism of progesterone regulation, the expression of key steroidogenic proteins—StAR, CYP11A1, and HSD3B-was analyzed in ovarian tissue across different time points. The StAR expression at 0h was significantly higher in the M+HE group compared with both NHE and HE groups (P<0.05; Fig. 2A). However, the difference between NHE and HE groups was not significant. By 16h, StAR levels decreased across all groups without significant differences (Fig. 2B). However, by 24h, the M+HE group exhibited a significant rebound in StAR expression, restoring it to levels comparable to 0h; the level was significantly higher in M+HE group than NHE and HE groups (P<0.05; Fig. 2C). CYP11A1 expression at 0h was significantly reduced in the HE and M+HE groups relative to the NHE group (P<0.05), the difference between former two groups was not significant (Fig. 2D). This reduction persisted at 16h across all groups, though the difference was not significant (Fig. 2E). By 24h, CYP11A1 expression in the M+HE group increased significantly in comparison with both HE and NHE groups (P<0.05), and the levels exceeded those observed at 0 and 16h (Fig. 2F). Regarding HSD3B, protein concentrations were significantly higher in the NHE group at 0h compared to both HE and M+HE groups (P<0.05; Fig. 2G); the difference between the latter two groups was not significant. Although all groups showed a reduction at 16h, no differences could be identified (Fig. 2H). Similarly, there were no significant variations in HSD3B expression among three groups at 24h (Fig. 2I).

Modulation of oxidative stress by melatonin in heat-exposed rats: Results of serum analysis revealed that at 0h of PGF injection, heat exposure significantly reduced serum SOD (Fig. 3A) and CAT activities (Fig. 3B) when compared with the NHE group (P<0.05). Melatonin treatment significantly enhanced SOD (Fig. 3A) and CAT (Fig. 3B) activities compared with the HE group (P<0.05). The HE group showed significantly higher MDA levels than NHE and M+HE groups (P<0.05; Fig. 3C), the difference between NHE and M+HE groups was not significant. Ovarian oxidative stress analysis indicated that at 16h post PGF injection, the HE group had significantly lower (P<0.05) SOD activity than the M+HE group. However, at 24h, SOD activity in the HE group was significantly lower than in both NHE and M+HE groups (P<0.05; Fig. 4A). In addition, at both points, the M+HE group showed significantly higher CAT levels than the HE group (P<0.05; Fig. 4B). MDA levels were significantly higher in the HE group in comparison with the NHE group (P<0.05). Meanwhile, MDA levels did not differ between the M+HE and HE groups at either time point (Fig. 4C).

Temporal alterations in RIPK1 and RIPK3 in rat ovaries during luteal regression post-PGF injection: Western blot analysis revealed distinct temporal patterns in the regulation of RIPK1 and RIPK3 proteins following PGF injection in NHE group. RIPK1 expression remained stable up to 8h post-injection but significantly increased at 16h (P<0.05), followed by a decline at 24h (P<0.05; Fig. 5A). Similarly, p-RIPK1 expression was significantly higher at 16h compared to baseline (P<0.05), with a reduction at 24h (Fig. 5B). The p-RIPK1/RIPK1 ratio remained stable until 8h but decreased significantly at both 16 and 24h (Fig. 5C). In contrast, RIPK3 protein levels exhibited a gradual increase, peaking at 24h post-PGF injection (P<0.05; Fig. 5D). The p-RIPK3 levels were elevated at 8h and remained significantly high through 24h (P<0.05; Fig. 5E). The p-RIPK3/RIPK3 ratio showed a significant decrease at both 2 and 24h post-injection compared with other time points (Fig. 5F).

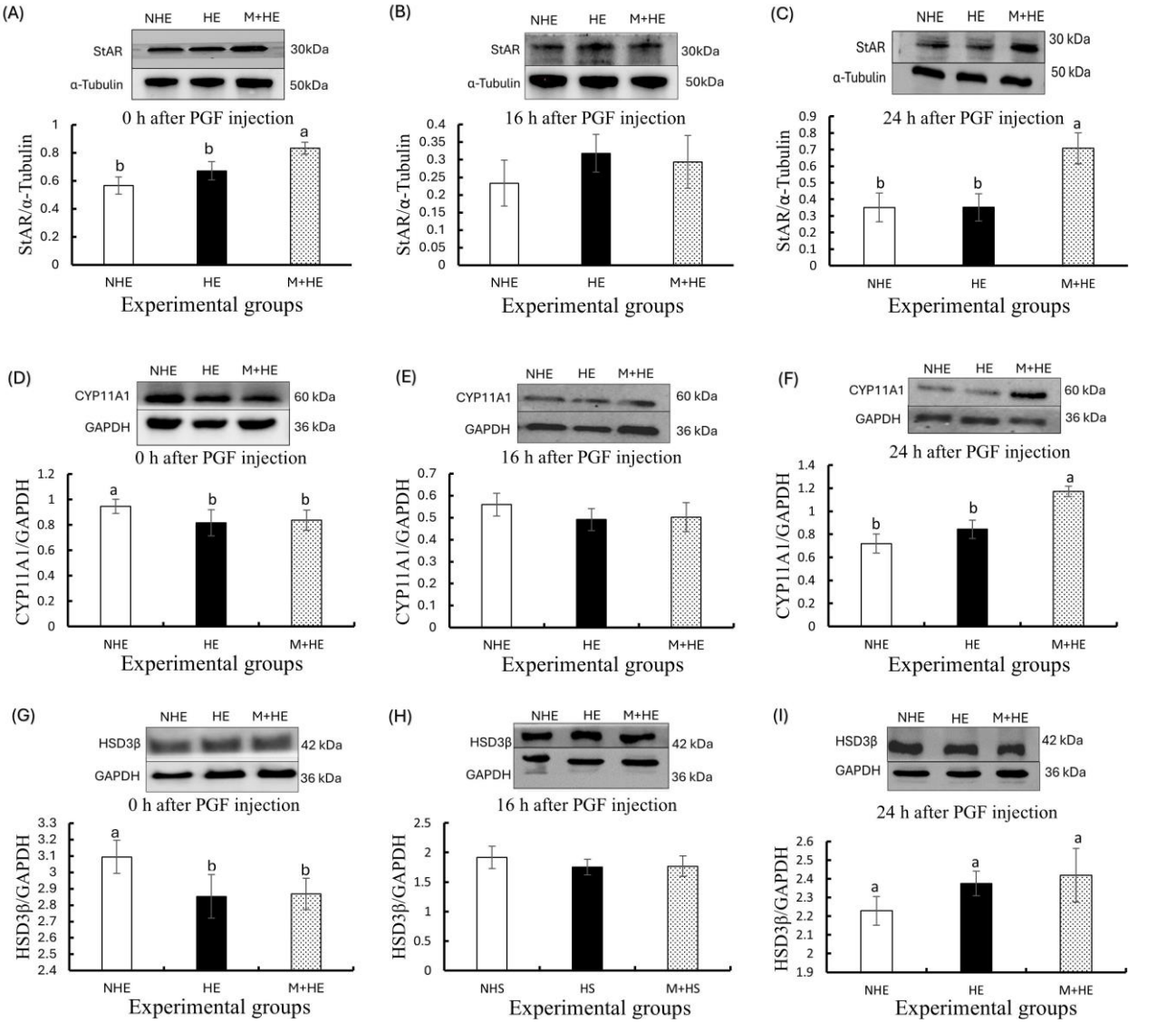

Fig. 2: Effect of melatonin and heat stress on steroidogenic protein expressions among NHE, HE and M+HE groups at different time points: (A-C) StAR, (D-F) CYP11A1 and (G-I) HSD3B at 0, 16, and 24h. The upper panel in each figure displays representative bands from the WB, whereas the lower panel presents the analysis of WB results using Image J. Data are presented as the mean±SEM of four rats. Different letters indicate significant differences (P<0.05) across groups.

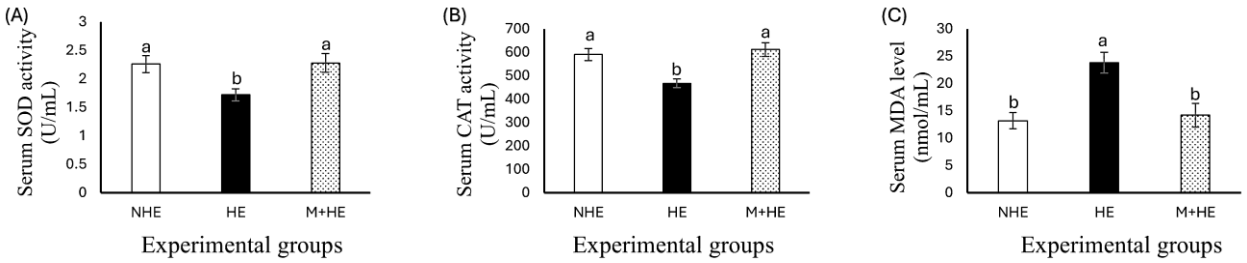

Fig. 3: Effect of melatonin on serum oxidative stress markers in heat-exposed rats. (A) SOD activity; (B) CAT activity; (C) MDA level. Significant differences are represented by different letters (P<0.05).

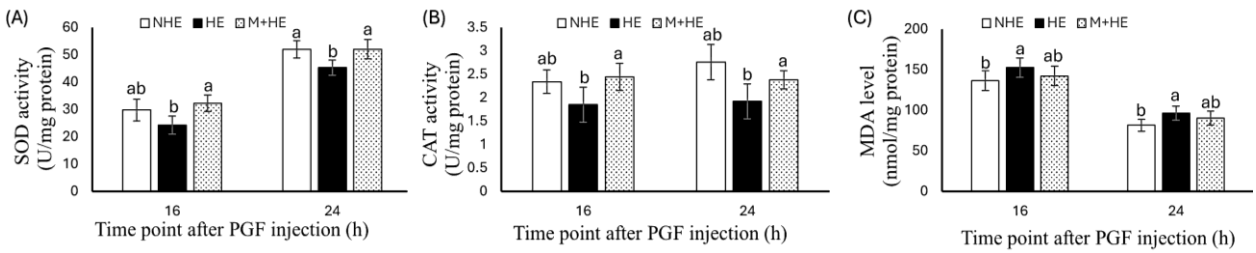

Fig. 4: Effect of melatonin on ovarian antioxidant capacity in heat-exposed rats post-PGF injection. (A) SOD activity; (B) CAT activity; (C) MDA level. Results are presented as the mean±SEM from three rats at each time point. Significant differences are represented by different letters (P<0.05).

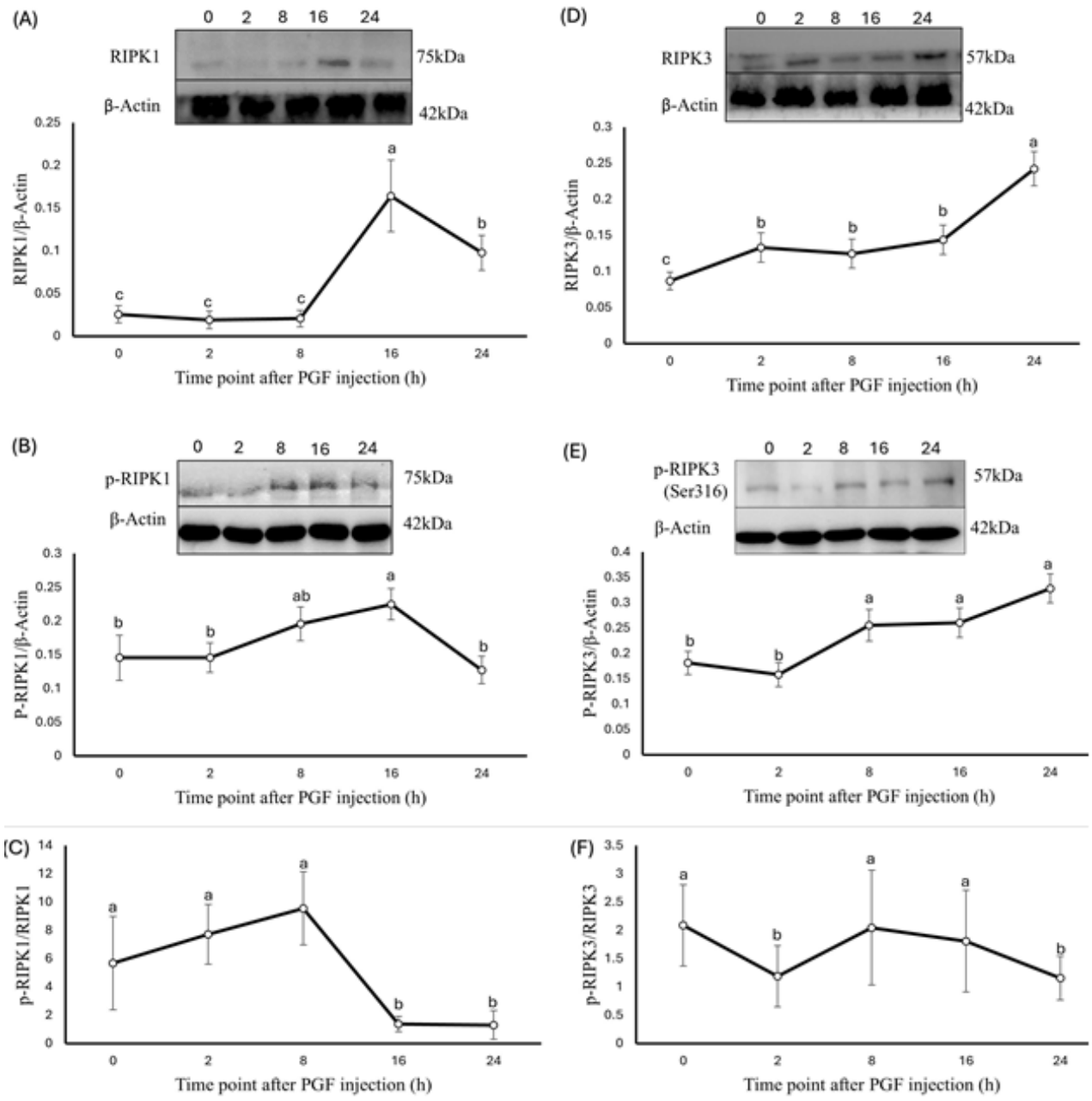

Fig. 5: Relative abundances of RIPK1, RIPK3 and their phosphorylation in rat ovaries after PGF injection in NHE group. (A) RIPK1, (B) p-RIPK1 protein expression levels, and (C) the p-RIPK1/RIPK1 ratio post-PGF. (D) RIPK3, (E) p-RIPK3 protein expression levels, and (F) the p-RIPK3/RIPK3 ratio post-PGF. Results are presented as mean±SEM from four rats per time point. Significant differences are represented by different letters (P<0.05).

Alteration of RIPK1 and RIPK3 in rat ovaries by melatonin and heat exposure post-PGF injection: Ovaries collected at 16 and 24h post-PGF injections were analyzed using WB to evaluate the expression of key necroptotic proteins, RIPK1 and RIPK3. These time points were selected based on previous findings highlighting the significant effects of heat exposure and melatonin on luteal function. At 16h, there were no significant variations in RIPK1 (Fig. 6A), p-RIPK1 (Fig. 6B) expression and p-RIPK1/RIPK1 ratio (Fig. 6C) across the groups. After 24h, heat exposure significantly up-regulated RIPK1 expression compared with the NHE group (P<0.05; Fig. 6D), while there were no variations among groups for p-RIPK1 (Fig. 6E) expression and p-RIPK1/RIPK1 ratio (Fig. 6F). Similarly, at 16h, there were no significant variations across groups in the expression of RIPK3 (Fig. 6G) and p-RIPK3/RIPK3 ratio (Fig. 6I). However, at this point, p-RIPK3 showed significantly higher expression in the HE than in M+HE group (Fig. 6H). In addition, at 24h, RIPK3 protein levels were significantly up-regulated in the HE group than in the M+HE group (P<0.05; Fig. 6M). Moreover, p-RIPK3 levels were up-regulated in HE compared with both NHE and M+HE groups (Fig. 6N), while the p-RIPK3/RIPK3 ratio was significantly higher in the HE group compared with the NHE group (P<0.05; Fig. 6O). The increased p-RIPK3/RIPK3 ratio in the HE group after 24h indicated that heat exposure activated necroptosis in ovarian cells. Melatonin administration significantly reduced RIPK3 phosphorylation levels compared with the HE group (P<0.05; Fig. 6N); however, it did not fully restore the p-RIPK3/RIPK3 ratio to the NHE group.

Localization of RIPK1 and RIPK3 in the corpus luteum post-PGF injection: Immunohistochemistry was used to visualize RIPK1 and RIPK3 protein expression at 16h post-PGF injection in luteal tissue. The results revealed positive staining for both RIPK1 (Fig. 7A) and RIPK3 (Fig. 7B) in the CL at this time point. However, quantitative analysis of the DAB staining score for both RIPK1 and RIPK3 across the different groups did not show any significant differences, indicating that the protein expression levels, while detectable, were not markedly altered between the groups at 16h.

Necroptosis in luteal cells from TEM analysis post-PGF injection: Transmission Electron Microscopy was employed to observe the ultrastructural changes characteristic of necroptosis in luteal cells 16h after PGF injection in the NHE group. Morphological changes indicative of necroptosis were identified, including

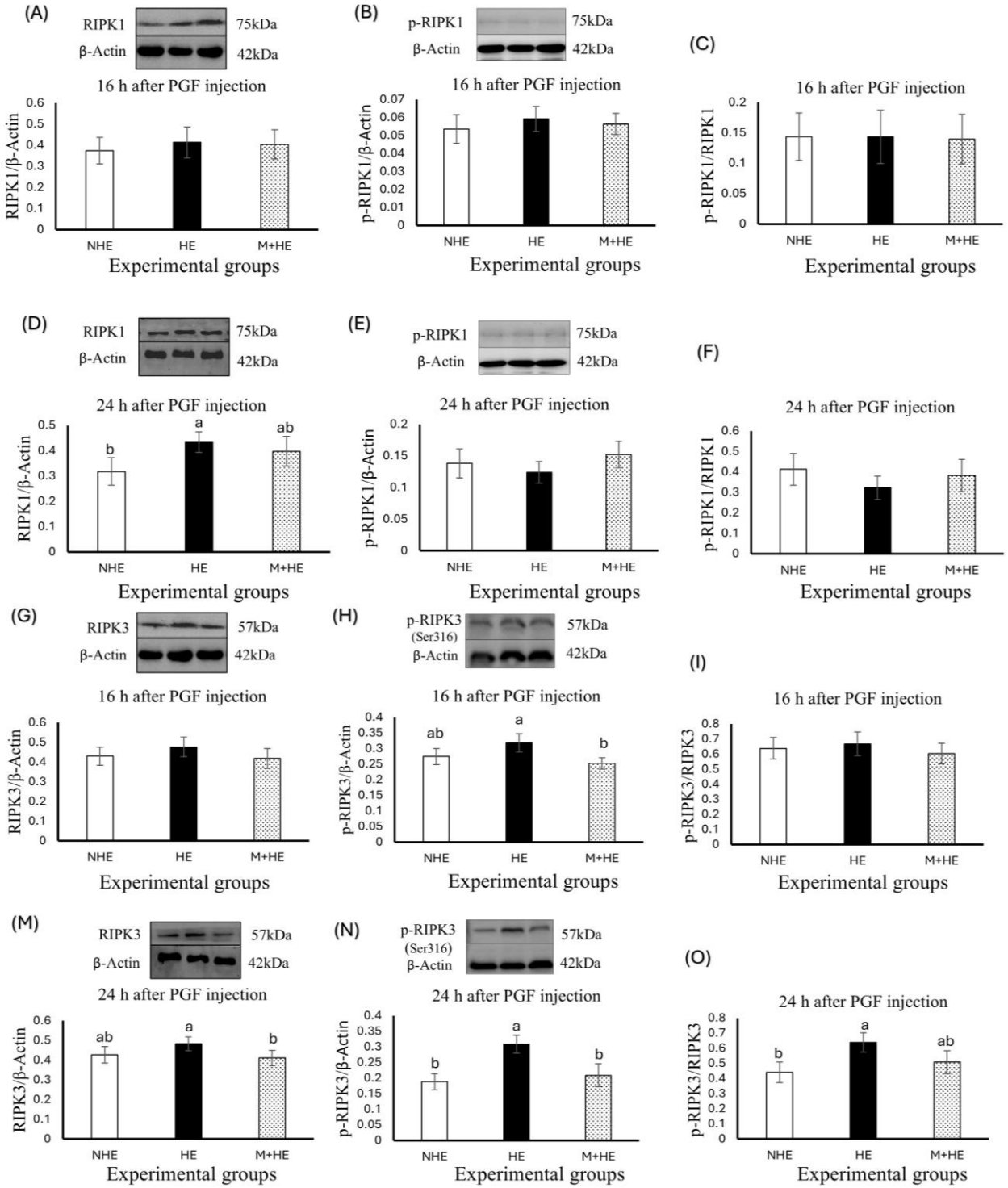

Fig. 6: Effects of heat exposure and melatonin administration on the protein expression of RIPK1, RIPK3, and their phosphorylation, in the rat ovaries following PGF injection. (A-C) Protein expression levels of RIPK1, p-RIPK1, and the p-RIPK1/RIPK1 ratio at 16h post -PGF; (D-F) Protein expression levels of RIPK1, p-RIPK1, and the p-RIPK1/RIPK1 ratio at 24h post-PGF. (G-I) Protein expression levels of RIPK3, p-RIPK3, and the p-RIPK3/RIPK3 ratio at 16h post-PGF; (M, N, O) Protein expression levels of RIPK3, p-RIPK3, and the p-RIPK3/RIPK3 ratio at 24h post-PGF. Results are presented as mean±SEM from four rats at each time point. Significant differences are represented by different letters ($P<0.05$).

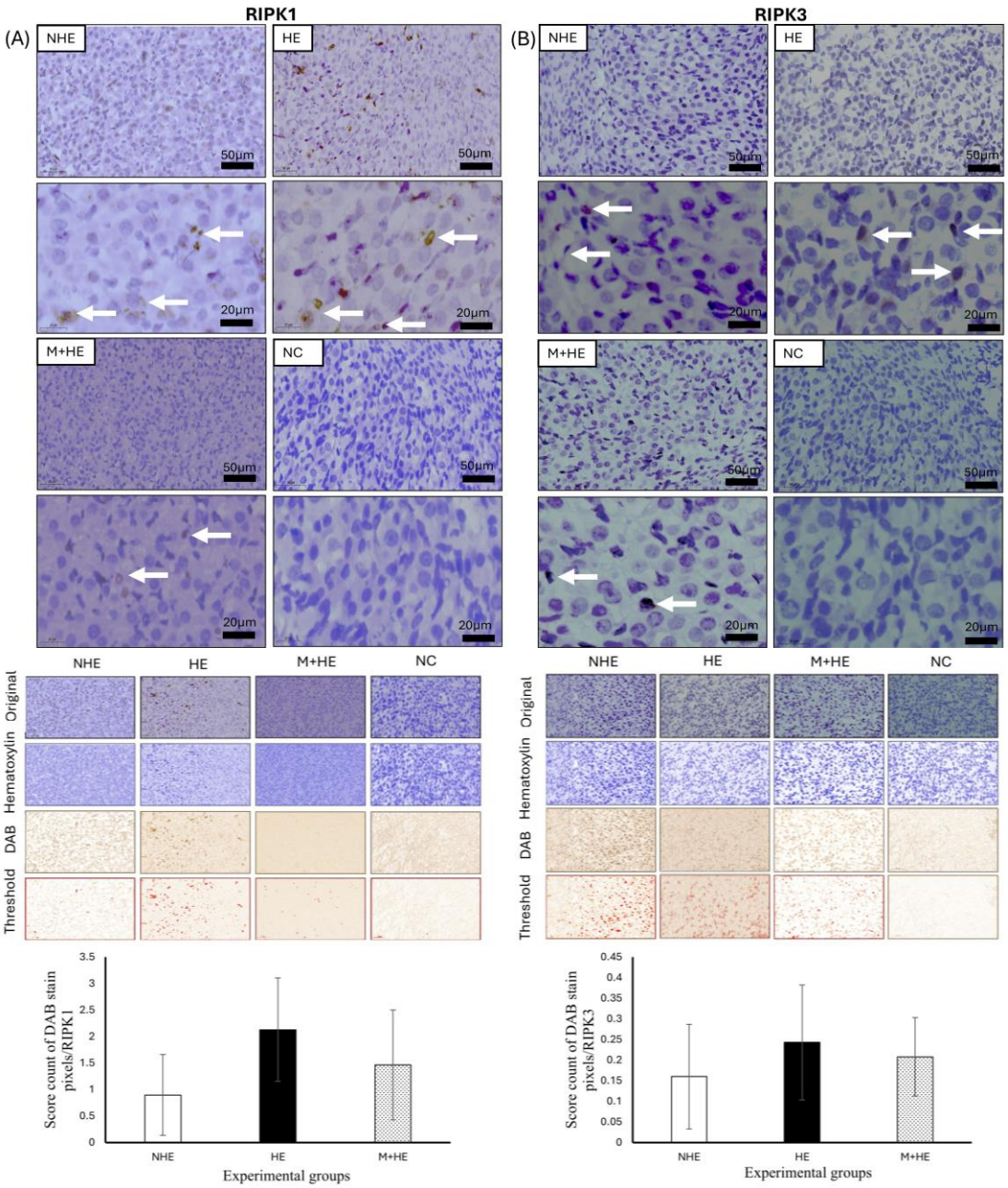

Fig. 7: Immunohistochemical and the localization of RIPK1 and RIPK3 proteins in the corpus luteum of rats 16h post-PGF injection. (A): RIPK1, (B): RIPK3, among different groups. NC indicates negative control. The upper panel of the figure displays the results of IHC, illustrating protein expression in the CL, using scale bar of 50 and 20μm. The middle panel presents Hematoxylin, DAB staining and threshold. The lower panel presents the quantitative analysis of the score count of DAB staining using Image J. Data are presented as means±SEM from three rats per time point.

Fig. 8: Morphological changes associated with necroptosis and apoptosis observed through transmission electron microscopy in large luteal cells (LLC) and small luteal cells (SLC) at16h post-PGF injection in NHE group. (A): Necroptosis; Chromatin regions appear densely packed and darker (condensed chromatin). The cytoplasm shows intact structures and organelles, indicating preservation without signs of rupture. However, rupture and permeabilization of the plasma membrane are evident, marked by white dashes, reflecting the loss of membrane integrity, a hallmark of necroptosis. Notably, there is an absence of nuclear condensation or fragmentation, which distinguishes necroptosis from apoptosis. (B): Apoptosis; Morphological changes include nuclear condensation and fragmentation, in contrast to necroptosis. The figure illustrates the distinct features of LLC and SLC, with annotations for the nucleus (N) and plasma membrane rupture (indicated by dashes). Scale bars=1μm and 500nm.

plasma membrane rupture and permeabilization, as highlighted by the presence of a white dash (Fig. 8A), reflecting the loss of membrane integrity, a hallmark of necroptosis. Notably, the necroptotic cells did not exhibit nuclear condensation or fragmentation, which are typical features of apoptosis. Instead, the apoptotic condensed chromatin and cytoplasm appeared intact, maintaining normal ultrastructure (Fig. 8B). These observations emphasize the distinct morphological characteristics of necroptosis as a unique type of programmed cell death.

DISCUSSION

The present study aimed to investigate the consequences of heat stress and melatonin in terms of oxidative stress, necrosis, and luteal function in the ovaries of rats after PGF injection, paying attention to the RIPK1 and RIPK3 signalization routes. Necroptosis is a form of programmed necrotic cell death regulated by phosphorylation of RIPK1. This mechanism leads to activation of RIPK3, which forms necrosomes and causes necrotic cell death in due course (Wegner *et al.*, 2017). The findings of this study revealed significant alterations in these pathways under heat stress conditions, underscoring the cytoprotective effects of melatonin in mitigating necroptosis and preserving luteal function.

The biphasic changes in serum progesterone levels were observed in this study; the current reduction at 2, 8 and 16h, followed by a rebound at 24h post-PGF injection, aligns with established patterns of luteal regression (Bai *et al.*, 2017; Qi *et al.*, 2018). Heat stress delayed progesterone suppression, possibly due to altered luteal metabolism or disruption of steroidogenic pathways. This may reflect impaired luteal cell function, consistent with previous reports of heat-induced reproductive disruptions (Han *et al.*, 2021). The results of this study also show that melatonin mitigates heat-induced elevations in progesterone levels, supporting the previous data that it enhances blastocyst development from heat-stressed bovine oocytes (Yaacobi-Artzi *et al.*, 2020). Moreover, melatonin up-regulates StAR and CYP11A1 expression to promote progesterone synthesis and to stabilize luteal function during luteal regression (Taketani *et al.*, 2011; Zhang *et al.*, 2018). Furthermore, melatonin promotes steroidogenic enzymes such as StAR and CYP11A1, resulting in facilitating progesterone synthesis and maintaining luteal stability during luteal regression (Liu *et al.*, 2020; Ratchamak *et al.*, 2022). These results emphasize the critical role of melatonin in protecting ovarian function under heat stress.

Apart from being an antioxidant, melatonin is also involved in hormone synthesis and maintenance of follicle health under stress. It influences the formation of reactive oxygen species or scavenge antioxidant activity, implicating a direct intervention on follicular growth and luteal function and may thereby provide a novel approach for enhancing reproductive performance under oxidative stress conditions.

In moderating the impact of heat stress, melatonin was observed to play a significant role. Melatonin also upregulated steroidogenic genes and proteins responsible for the biosynthesis of progesterone during luteal regression. These results are consistent with the previous preclinical studies indicating that melatonin enhances progesterone synthesis during luteinization and modulates steroidogenesis, particularly under conditions of stress (Taketani *et al.*, 2011; Zhang *et al.*, 2018). The ability of melatonin to maintain the function of luteal cells during heat stress suggests its possible use as a therapeutic compound for the protection of reproduction under adverse environmental conditions.

Compared to NHE rats, heat exposure did not affect basal levels of progesterone, which is in agreement with other bovine investigations showing that heat stress has no effect during the follicular phase (Sammad *et al.*, 2020). The observed delay in progesterone suppression during heat stress indicates that heat affects luteal cell metabolism and may alter steroid pathways. The failure of progesterone to decline promptly after PGF treatment in heat stress signals disturbance in normal patterns of luteal regression, potentially due to changes in microenvironmental factors or could have been provoked by affecting heat stress or direct effects on steroidogenic enzymes. This observation is in agreement with increased progesterone levels observed during the estrus when environmental temperature was high (Han *et al.*, 2021).

Oxidative stress is a well-established contributor to necroptosis and intracellular damage in different body organs, including organs of reproductive system (Sengul *et al.*, 2021; Kükürt and Karapehlivan, 2022). The current heat-induced increase in serum MDA and decrease in SOD and CAT activities probably promoted necroptosis through the RIPK1/RIPK3 pathway, since the RIPK3 phosphorylation was enhanced following exposure to heat stress. The activities of these kinases in necroptotic signaling at 16h after the PGF administration suggest their function in luteal regression through oxidative stress and necroptosis.

The antioxidant effects of melatonin were further supported by its ability to decrease the oxidative injury caused by heat. The observed increase in activities of SOD and CAT, and decrease in the MDA level in NHE and M+HE groups compared with HE group, is in accordance with the results of previous studies that melatonin strengthens the cellular antioxidant defense system to reverse oxidative stress (Ziaadini *et al.*, 2017; Reina and Martínez, 2018). Furthermore, the suppression of RIPK3 and p-RIPK3 by melatonin in heat-shocked ovaries suggests that melatonin may participate in the necroptotic signaling pathway, preventing oxidative stress and maintaining luteal integrity.

The temporal regulation of RIPK1 and RIPK3 proteins revealed distinct patterns of necroptosis activity during luteal regression. Notably, at 2 and 8h post-PGF injection, minimal alterations in necroptotic markers and oxidative stress indices were observed, indicating that these time points represent early phases of luteal regression with limited impact. The 0-h samples served as baseline controls for comparison. In contrast, pronounced effects of heat stress and melatonin treatment were evident at 16 and 24h post-PGF injection, which correspond to the critical biologically active phases of PGF-induced luteal regression. These later time points revealed significant modulation of necroptotic pathways and oxidative stress markers, highlighting the temporal dynamics of luteal response to stress and therapeutic

intervention. Heat treatment was discovered to raise the levels of RIPK1 and RIPK3 and their phosphorylated forms most evidently at 24h post-PGF injection in our study. As shown in previous studies, the regulation of the RIPK1/RIPK3 signaling pathway is critical for necroptosis during the luteal regression under high-temperature conditions (Wegner *et al.*, 2017). Under conditions of heat stress, the increased p-RIPK3/RIPK3 ratio in heat-stressed ovaries indicates higher necroptotic activity and subsequently disintegration of luteal cells

The current melatonin-induced decrease in the p-RIPK3 and RIPK3, especially at 24h, indicates the ability of melatonin to reduce necroptotic signaling in heat-affected ovaries. The ability of melatonin to reduce phosphorylated RIPK3 levels thus suggests partial inhibition of necroptosis, which is particularly important for protecting the luteal function and enhancing cell survival when they are exposed to heat stress conditions. Melatonin inhibited phosphorylation of RIPK1 and RIPK3 levels, which strongly suggests its critical role in preventing necrosome complex formation and necroptosis propagation. Melatonin reduced the p-RIPK3 signaling, which decreased cell death and maintained the luteal microenvironment conducive to steroid production and support of ovarian function during luteal regression.

Conclusions: In conclusion, melatonin plays a crucial role in regulating necroptotic processes and strengthening antioxidant defenses. By enhancing luteal steroid production, it offers a comprehensive prophylactic strategy for preserving ovarian function under environmental stress conditions. These findings align with existing literature, supporting the potential of melatonin as an effective therapeutic option to improve reproductive performance in pregnant females exposed to high levels of heat stress.

Conflict of interest: The authors declare that they have no conflict of interest.

Authors contribution: TH conceived the study idea, managed the methodology and together with SU, arranged the necessary software. Validation was performed by TM, YH, SU, and WE, while resources were provided by YH and WE. TH drafted the manuscript, which was critically reviewed and collaboratively edited by TH, TM, YH, SU, WE and DM. Visualization was handled by TH and SU, with DM providing overall supervision. All authors contributed to data interpretation, provided significant intellectual input, and approved the final version for publication.

Funding: This work was financially supported by the National Natural Science Foundation of China (32072727).

REFERENCES

Ahmad SB, Ali A, Bilal M, *et al.*, 2023. Melatonin and health: Insights of melatonin action, biological functions, and associated disorders. Cell Mol Neurobiol 43(6):2437-58.

Bai WJ, Jin PJ, Kuang MQ, *et al.*, 2017. Temporal regulation of extracellular signal-regulated kinase 1/2 phosphorylation, heat shock protein 70, and activating transcription factor 3 during prostaglandin F2α-induced luteal regression in pseudopregnant rats following heat stress. Reprod Fertil Dev 29(6):1184-93.

Butt MA, Shahid MQ, Bhatti JA, *et al.*, 2019. Effect of dietary vitamin E and selenium supplementation on physiological responses and reproductive performance in Holstein Friesian bulls during humid hot summer. Pak Vet J 39(4):593-97.

Chrustek A and Olszewska-Slonina D, 2021. Melatonin as a powerful antioxidant. Acta Pharm 71(3):335-54.

Góes L, Vilarino F, Oba E, *et al.*, 2022. Review of the literature on corpus luteum insufficiency in women (2015–2020) and in domestic animals (1980–2020). Clin Investig Ginecol Obstet. 49(2):100724.

Hadwan MH, Hussein MJ, Mohammed RM, *et al.*, 2024. An improved method for measuring catalase activity in biological samples. Biol Methods Protoc 9(1):bpae015: doi: 10.1093/biomethods/bpae015.

Han J, Yang D, Liu Z, *et al.*, 2021. The damage effect of heat stress and psychological stress combined exposure on uterus in female rats. Life Sci 286: 120053.

Hojo T, Piotrowska-Tomala KK, Jonczyk AW, *et al.*, 2019. Receptor interacting protein kinases-dependent necroptosis as a new, potent mechanism for elimination of the endothelial cells during luteolysis in cow. Theriogenology 128:193-200.

Hojo T, Skarzynski DJ and Okuda K, 2022. Apoptosis, autophagic cell death, and necroptosis: different types of programmed cell death in bovine corpus luteum regression. J Reprod Dev 68(6):355-60.

Huang X, Tan S, Li Y, *et al.*, 2021. Caspase inhibition prolongs inflammation by promoting a signaling complex with activated RIPK1. J Cell Biol 220(6):e202007127.

Jiang Y, Shi H, Liu Y, *et al.*, 2021. Applications of melatonin in female reproduction in the context of oxidative stress. Oxid Med Cell Longev 2021:6668365.

Jiao H, Wachsmuth L, Kumari S, *et al.*, 2020. Z-nucleic-acid sensing triggers ZBP1-dependent necroptosis and inflammation. Nature 580(7803):391-95.

Krishnan G, Bagath M, Pragna P, *et al.*, 2017. Mitigation of the heat stress impact in livestock reproduction. In: "Carreira RP (Ed), Theriogenology" 1st ed, Intech International Publisher pp:64-86.

Kükürt A and Karapehlivan M, 2022. Protective effect of astaxanthin on experimental ovarian damage in rats. J Biochem Mol Toxicol 36(3):e22966.

Liu XC, Sun TC, Li HY, *et al.*, 2020. Antioxidative effect of melatonin on cryopreserved ovarian tissue in mice. Cryobiology 91:99-105.

Mojaverrostami S, Asghari N, Khamisabadi M, *et al.*, 2019. The role of melatonin in polycystic ovary syndrome: A review. Int J Reprod Biomed 17(12):865-82.

Monaco CF and Davis JS, 2023. Mechanisms of angioregression of the corpus luteum. Front Physiol 14:1254943.

Morgan MJ and Kim YS, 2022. Roles of RIPK3 in necroptosis, cell signaling, and disease. Exp Mol Med 54(10):1695-704.

Nanas I, Chouzouris TM, Dovolou E, *et al.*, 2021. Early embryo losses, progesterone, and pregnancy associated glycoproteins levels during summer heat stress in dairy cows. J Therm Biol 98:102951.

Pate JL and Hughes CHK, 2023. Luteal prostaglandins: mechanisms regulating luteal survival and demise in ruminants. Animal 17:100739.

Qi L, Guo N, Wei Q, *et al.*, 2018. The involvement of NR4A1 and NR4A2 in the regulation of luteal function in rats. Acta Histochem 120(8):713-19.

Ratchamak R, Thananurak P, Boonkum W, *et al.*, 2022. The melatonin treatment improves the ovarian responses after superstimulation in Thai-Holstein crossbreeds under heat stress conditions. Front Vet Sci 9:888039.

Reina MM and Martínez A, 2018. A new free radical scavenging cascade involving melatonin and three of its metabolites (3OHM, AFMK, and AMK). Comput Theor Chem 1123:111-18.

Reiter RJ and Sharma R, 2021. Central and peripheral actions of melatonin on reproduction in seasonal and continuous breeding mammals. Gen Comp Endocrinol 300:113620.

Sammad A, Umer S, Shi R, *et al.*, 2020. Dairy cow reproduction under the influence of heat stress. J Anim Physiol Anim Nutr 104(4):978-86.

Sengul E, Gelen V and Gedikli S, 2021. Cardioprotective activities of quercetin and rutin in Sprague Dawley rats treated with 5-fluorouracil. J Anim Plant Sci 31(2):423-31.

Taketani T, Tamura H, Takasaki A, *et al.*, 2011. Protective role of melatonin in progesterone production by human luteal cells. J Pineal Res 51(2):207-13.

Tang Z, Chen J, Zhang Z, *et al.*, 2021. HIF-1α activation promotes luteolysis by enhancing ROS levels in the corpus luteum of pseudopregnant rats. Oxid Med Cell Longev 2021:1764929.

Ullah S, Zhang M, Yu H, *et al*., 2019. Heat exposure affected the reproductive performance of pregnant mice: Enhancement of autophagy and alteration of subcellular structure in the corpus luteum. Reprod Biol 19(3):261-69.

Vandenabeele P, Galluzzi L, Vanden Berghe T, *et al*., 2010. Molecular mechanisms of necroptosis: an ordered cellular explosion. Nat Rev Mol Cell Biol 11(10):700-14.

Wegner KW, Saleh DD and Degterev A, 2017. Complex pathologic roles of RIPK1 and RIPK3: moving beyond necroptosis. Trends Pharmacol Sci 38(3):202-25.

Yaacobi-Artzi S, Shimoni C, Kalo D, *et al*., 2020. Melatonin slightly alleviates the effect of heat shock on bovine oocytes and resulting blastocysts. Theriogenology 158:477-89.

Yang J, Cao Y and Zhang N, 2020. Spectrophotometric method for superoxide anion radical detection in a visible light (400–780 nm) system. Spectrochim Acta Part A: Mol Biomol Spectrosc 239:118556.

Yang Z, Li C, Wang Y, *et al*., 2018. Melatonin attenuates chronic pain-related myocardial ischemic susceptibility through inhibiting RIP3-MLKL/CaMKII-dependent necroptosis. J Mol Cell Cardiol 125:185-94.

Yong W, Ma H, Na M, *et al*., 2021. Roles of melatonin in the field of reproductive medicine. Biomed Pharmacother 144:112001.

Yu H, Zhao J, Pei X, *et al*., 2023. Dual role of NR4A1 in porcine ovarian granulosa cell differentiation and granulosa-lutein cell regression in vitro. Theriogenology 198:292-304.

Zhang W, Wang Z, Zhang L, *et al*., 2018. Melatonin stimulates the secretion of progesterone along with the expression of cholesterol side-chain cleavage enzyme (P450scc) and steroidogenic acute regulatory protein (StAR) in corpus luteum of pregnant sows. Theriogenology 108:297-305.

Zhou H, Li D, Zhu P, *et al*., 2018. Inhibitory effect of melatonin on necroptosis via repressing the Ripk3-PGAM5-CypD-mPTP pathway attenuates cardiac microvascular ischemia–reperfusion injury. J Pineal Res 65(3):e12503.

Ziaadini F, Aminae M, Rastegar MM, *et al*., 2017. Melatonin supplementation decreases aerobic exercise training-induced lipid peroxidation and malondialdehyde in sedentary young women. Pol J Food Nutr Sci 67(3):225-32.